Mining of Mineral Deposits
Volume 20 (2026), Issue 1, 41-51

https://doi.org/10.33271/mining20.01.041

Numerical simulation of quarry wall stability considering the fault location in the bottom part

Asangiz Moldabayev [1], Dmytro Babets [2], Serik Moldabayev [1], Olena Sdvyzhkova [2*], Atac Bascetin [3], Zhanat Sultanbekova [1]

[1] *Satbayev University, Almaty, Kazakhstan*
[2] *Dnipro University of Technology, Dnipro, Ukraine*
[3] *Istanbul Technical University, Istanbul, Turkey*

**Corresponding author: e-mail sdvyzhkova.o.o@nmu.one*

Abstract

Purpose. The research aims to assess the impact of geological disturbances located in the bottom part of the super-deep Kacharsky Ore Quarry on the stress-strain state (SSS) of its walls and to determine the safety factor of the walls, taking into account the complex geological situation.

Methods. Fault plane modelling methodology is based on 3D finite-element analysis using the RS3 Rocscience software. Fault zone is represented by a medium with a system of fractures. Fracture characteristics, such as openness, contact filler type, and surface quality are achieved by selecting the normal and shear stiffness of the contact. The strength and deformation properties of rock inside the fault zone are defined by low geological index values (GSI = 20), corresponding to the "poor" quality mass according to the Hoek-Brown classification. The main mass outside the fault zone is represented by elastic-plastic medium, where the transition to inelastic deformation stage is determined by the Mohr-Coulomb failure criterion.

Findings. FEM-analysis of the stress-strain state of the Kacharsky quarry walls at various stages of mining, taking into account faults in its bottom part, provides a safety factor (FoS) that is 28-30% lower than that obtained without considering the faults. Parametric analysis shows that for normal stiffness values of the fracture-filling material up to 2.5 GPa/m, the difference in the realized shear strains is most significant. When the *Er* index, which characterizes the ratio of material stiffness inside and outside the fault zone, decreases from $E_r = 0.2$ to $E_r = 0.05$, the maximum shear strains in the bottom part of the quarry increase from 0.05 to 0.075, that is, by 50%. Thus, a weaker and more disintegrated medium in the fault zone provokes the development of shear strains and causes a decrease in the stability of the walls.

Originality. For the first time, under real mining-geological conditions of deep ore quarry, a pattern of change in safety factor of steeply sloping walls has been identified, taking into account geological faults in the bottom part of the quarry. A dependence of shear strains on the normal stiffness index of fractures and the ratio of stress-strain modules of the rock medium inside and outside the fault zone has been found.

Practical implications. The wall safety factor (FoS) value at each stage of mining is a key parameter for adoption of technological decisions and regulations. The established fact that the stability of the walls has decreased to a critical level (FoS = 1.1) at the final stage of mining due to the presence of faults may serve as a basis for revising the technological scheme of ore mining at the final stage, in particular, to reduce the slope angle of the benches.

Keywords: *geological fault; open-pit mining; deep quarry; slope stability; numerical modelling*

1. Introduction

Open-pit mining continues to be the dominant trend in the development of the mining industry worldwide. However, with the increase in the mining depth and the slope angle of the quarry walls, ensuring the stability of walls, and, consequently, the safety of workers, has become more complicated [1]. Mining also causes large-scale disturbance of the earth's surface and requires integrated approaches to improve the state of mining-affected territories [2].

A sound prediction of slope stability is a crucial issue when planning a quarry wall, both in soil and rocks [3], [4]. Probabilistic and rating-based approaches for rock mass stability assessment are increasingly applied in deep mining conditions [1], [5].

Rock masses are the product of long-term geological processes, including tectonic ones. This leads to the rock mass having structural peculiarities such as discontinuities, which are called faults. The interaction between the stress field in the upper part of the Earth's crust and pre-existing faults is a critical issue in geomechanics [6]-[8], since the value and orientation of the natural stress field directly determine the stability of rock outcrops during mining [9], [10].

Received: 31 October 2025. Accepted: 19 February 2026. Available online: 30 March 2026

Mining of Mineral Deposits. ISSN 2415-3443 (Online) | ISSN 2415-3435 (Print)

A cluster of several parallel faults forms a fault zone. However, this term is also used to refer to an area of fragmented rock along a single fault. Long-term displacement of rocks along closely spaced faults can blur the boundaries between them, as the rock between the faults is converted into rock lenses and then gradually crushed [11]. Many scientists have studied the properties of discontinuities and their impact on the stability of natural slopes and quarry walls [12]-[14]. It should be noted that quarry walls often comprise several rock layers, many of which are relatively weak and disturbed by faults [15]. The authors emphasize that mining operations near faults can have a radical impact on the stability of nearby areas. A typical example of this is the Mavropigi open-pit lignite complex in north-western Greece, where discontinuous faults occurred at a depth of 150 m near the excavation and created serious problems for the stability of the quarry walls [16]. Faults often form rock blocks that become unstable when mined, causing local caving. This case is described in detail in [17].

Later works also focus on studying the influence of multiple faults on the stability of steep and very steep slopes in quarries. In [18], a joint assessment was conducted to analyze the stability of steep slopes under the combined influence of four faults at the Tan Ya limestone mine owned by Gezhouba Xing Shan Cement Co. The assessment covered the current state of fault development and the characteristics of damage associated with slope instability during subsequent deep mining. The finite difference method implemented in the FLAC3D software code was used to model faults. The results show that the presence of faults determines the shape of slope damage in the Tan Ya quarry, which in turn affects slope stability. The mechanical cause of slope damage is a fault passing through the rock mass, which leads to a relative shear and extrusion of rock in the fault zone. In [19], it is indicated that understanding how stress is redistributed during shear is extremely important for assessing the risks associated with faults. This study uses a discrete element method to model fault activation and stick-slip sliding, as confirmed by laboratory experiments. The numerical model takes into account stress changes on fault planes, stress field distribution in surrounding rock masses, as well as local stress and fracture development in the fault zone. The modelling results show that sliding along the fault causes stress redistribution, which is primarily characterized by a change in the direction of the principal stress near the fault and heterogeneity in stress distribution.

The authors in [20] indicate that fault reactivation is a dynamic, non-equilibrium process. As the rock mass gradually collapses, the stress field in the fault zone is redistributed, resulting in the fault reactivation. This process further exacerbates damage to the rock mass, leading to a steady increase in permeability coefficient in the fault zone, thereby increasing the probability of water ingress into the mined-out space. The peculiarities of fault reactivation here are associated with water seepage and, consequently, with changes in contact conditions at the boundary of fractures in the fault zone.

Analysis of publications shows that it is extremely important to study how faults affect the stability of the surrounding soil-rock mass, focusing both on fault activation criteria [21], and on quantitative assessments of the influence of faults on the stability of rock outcrops [22]. Recent studies also analyse the stress-strain state of the near-wall rock mass in deep quarries to improve stability management strategies [23].

The purpose of this paper is to assess the influence of faults located in the bottom part of the quarry on the wall stability during the sequential removal of steeply sloping ore layers, based on mathematical modelling of these complex geological structures.

Since modelling a large-scale discontinuity in solids is a very complex task in solid mechanics, researchers mainly use two-dimensional (2D) slope analysis with numerical methods, including the finite element method (FEM). As a rule, the result of the analysis is only the local stability of that slope area where the fault has formed. However, most natural disasters, such as slope landslide and quarry wall caving, occurring in practical engineering, are caused by the state of the entire three-dimensional (3D) area where mining operations are carried out. Therefore, in complex geological conditions, the results of two-dimensional numerical modelling will differ significantly from the actual situation. Three-dimensional analysis of the stress-strain state (SSS) of the rock mass near the outcrop, in particular around the quarry bowl, taking into account the localization of faults, will more realistically reflect the stability of the quarry walls [25], [26]. With the development of computer technology, more and more researchers use the FEM in 3D setting to assess slope stability and study the mechanism of their failure. However, the issue of the influence of faults on slope stability in a 3D setting has not been sufficiently explored, as noted by the authors in [27], [28].

An important issue requiring discussion is the method of mathematical modelling of solid-body discontinuity. In geomechanics, a fault is considered to be an internal displacement discontinuity that allows slippage along the discontinuity surfaces. The description concept of Mohr-Coulomb shear strength is applied in terms of cohesion and internal friction angle [29]. It is a well-known fact that the physical-mechanical properties of rocks in the fault zone differ significantly from those characteristic of the rest of the mass. This heterogeneity determines the influence of the fault zone on the stress field near the fault zone, along with the complex fault geometry, as shown in [30].

The authors of papers [31], [32], considering faults as three-dimensional structures with different material properties in different areas of the fault zone, developed a concept known as “fault facies”. It is believed that the volume inside the fault can be filled with a special facies, which is similar in properties to weak sedimentary rocks. When using a continuous approach, the fault is modelled using specially selected elements with modified properties, such as reduced Young’s modulus, plastic or viscous behaviour. In contrast, in a discrete approach, the fault is represented by contact elements that allow displacement along the boundaries of these structures [33].

The authors in [34] used various mechanical properties to describe the fault zone, distinguishing between the host rock, the damage zone, and the fault core. The numerical model uses contact elements for which the Young’s modulus and friction coefficient vary. In addition, the angles of dip and strike of the fault vary. The results showed that the stress tensor outside the fault core depends significantly on the fault friction coefficient, rock strength, and fault stiffness. The greatest influence of the fault on stress values and stress tensor orientation is observed at a distance of 1000 m from the fault boundaries.

This paper also uses a finite-element model of a rock mass with a complex structure, which includes an open-pit mining and a fault zone in the bottom part of the quarry. The purpose of modelling is to determine the influence of fault on the wall stability of the super-deep round-shaped quarry.

2. Materials and methods

2.1. Object of research

The Kacharsky quarry, one of the largest iron ore quarries in Kazakhstan, is located in the Kostanay Region. Ore deposits here extend to a depth of more than 1 km. Magnetite predominates in the composition of the ores, but pyrite, chalcopyrite, sphalerite and other minerals are also found. The quarry is almost circular in shape (Fig. 1) and has an actual depth of 570 m.

Figure 1. View of the Kacharsky quarry (Google Earth)

Ore mining in the quarry is conducted with steeply sloping layers from top to bottom. The removal of each i-th steeply sloping layer ($i = 1, n$) is considered as a stage in mining of the ore body. The planned depth of the quarry is achieved by organizing 25 stages ($n = 25$). Figure 2 shows the contours of the first nine stages of mining on a section of the eastern wall of the quarry. It is during these stages that the boundary contours of the quarry on the surface are reached.

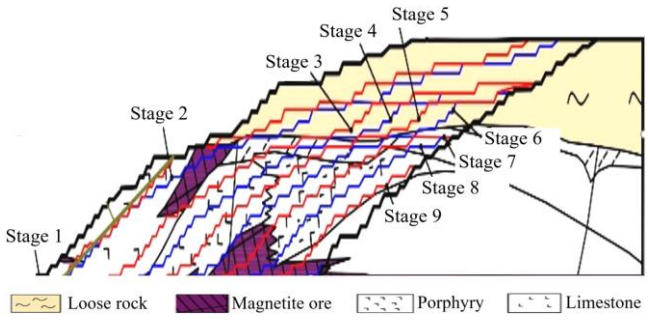

Figure 2. Quarry wall fragment showing the contours of the first nine mining stages

The layers of rock overburden differ in their mechanical properties, but a height of 15 m and a slope angle of 70° are adopted for all benches. Double benches and safety berms 5 m wide are also used. The width of the working platforms is 60 m. The most important parameter of mining, influencing both the efficiency of operations and their safety, is the resulting slope angle of the wall, which is formed by a line of benches, working platforms and berms. At each stage of mining, the depth increases and the wall slope angle increases, which, together with the strength properties of the rock, controls the wall stability. In [35], the stability of walls at each stage of mining was assessed using both 2-D and 3-D finite element models, taking into account both the structure of the rock mass and the possible statistical variation of properties within the rock layer. Despite the fact that all previous calculations predicted a sufficiently stable state of the wall even at the final stage of mining, there is concern about the fact that a fairly large geological fault has been identified in the bottom part of the quarry (Fig. 3). It creates additional zones of weakening and, consequently, causes a redistribution of stresses as the quarry deepens.

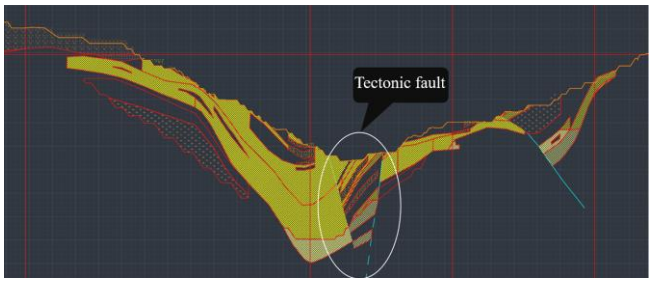

Figure 3. Digital model of a quarry rock mass in the vicinity of an open pit excavation, with emphasis on the geological fault zone

Changes in the stress-strain state of rocks in the area of lower benches may influence the overall wall stability. Therefore, in this paper, we focused specifically on modelling the geological fault zone in order to assess its influence on the formation of potential shear strains and sliding surfaces in the quarry walls.

2.2. Method for modelling rock mass SSS

It was mentioned above that one of the effective methods for modelling geomechanical processes in rock masses with complex structures is FEM. Rocscience's RS3 software, implementing FEM in a 3-D setting, was used to determine the SSS components of the rock mass area covering the entire Kacharsky quarry bowl.

The digital contours of the quarry were initially created in Surpac software and implemented in the RS3 calculation module. The area including the quarry bowl is divided into tetrahedral finite elements. The calculation scheme assumes that there are no displacements along the XY plane (bottom of the model), that is, the plane is fixed along the X, Y and Z axes; the YZ plane is fixed along the X and Y axes; the XZ plane is fixed along the Y axis (Fig. 4).

Due to the large volume of the finite element model (more than 3000 tetrahedral finite elements), at this stage of research, a homogeneous mass was modelled, to which average properties characteristic of limestone were assigned, since layers of this rock dominate in the rock mass structure.

The homogeneous rock mass has the following average physical-mechanical properties: cohesion 475 kPa, internal friction angle 36°, Poisson's ratio 0.27, Young's modulus 2.65 GPa. The absence of layer boundaries reduces the number of elements in the finite element mesh and allows you to focus on accurately reproducing the line of the quarry wall benches. An idealized rock medium is modelled for the purity of the computational experiment to exclude the influence on the SSS of layers with different stiffness. This makes it possible to assess the influence of fault boundaries on the quarry wall stability.

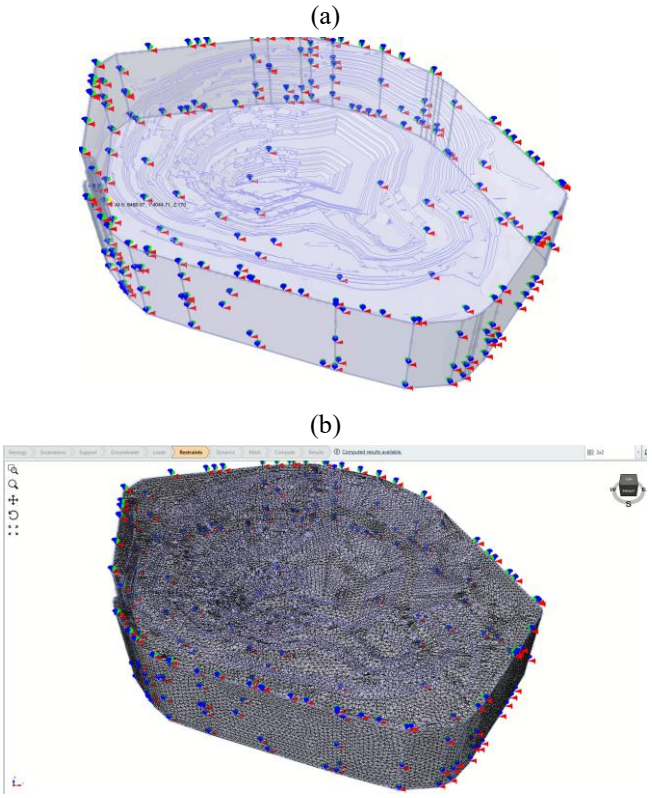

Figure 4. Designed (a) and finite element (b) model schemes

The main quantitative indicator of quarry wall stability is the safety factor (FoS), which is generalized in the Expression:

$$\mathrm{FOS} = \frac{\int \left(C + \sigma \tan \varphi\right) dA}{\int \tau dA}, \quad (1)$$

where:

C and φ – cohesion and internal friction angle, respectively;

σ – normal stress;

τ – shear strength;

A – sliding surface area [36].

To combine the FoS concept with a numerical approach, the Shear Strength Reduction method is used. To do this, two additional shear strength parameters C_R and φ_R are introduced, obtained by dividing the actual shear strength parameters C and φ by the Strength Reduction Factor (SRF). By stepwise modification of SRF, a set of C_R and φ_R is generated for finite element calculations. The value of SRF, at which the finite element model collapses, that is, solution of the constitutive equation system diverge, is assumed to be equal to the safety factor (FoS). Therefore, we will continue to use the SRF parameter as a stability indicator, understanding it to mean the safety factor.

2.3. Geological fault modelling

For direct modelling of the tectonic fault, a plane coinciding with the strike of the fault is added to the finite element model. This plane is a discontinuity surface along the edges of which sliding is possible. The RS3 software utilizes the "Add Joint Surface" function. The modelled surface intersects part of the domain geometry and divides the external volume in accordance with the specified edge conditions. In essence, this surface is the fault core (Fig. 5), which is most often accompanied by feathering fracturing, that is, it is surrounded by a damaged rock zone that extends 30-60 m from the fault core [37].

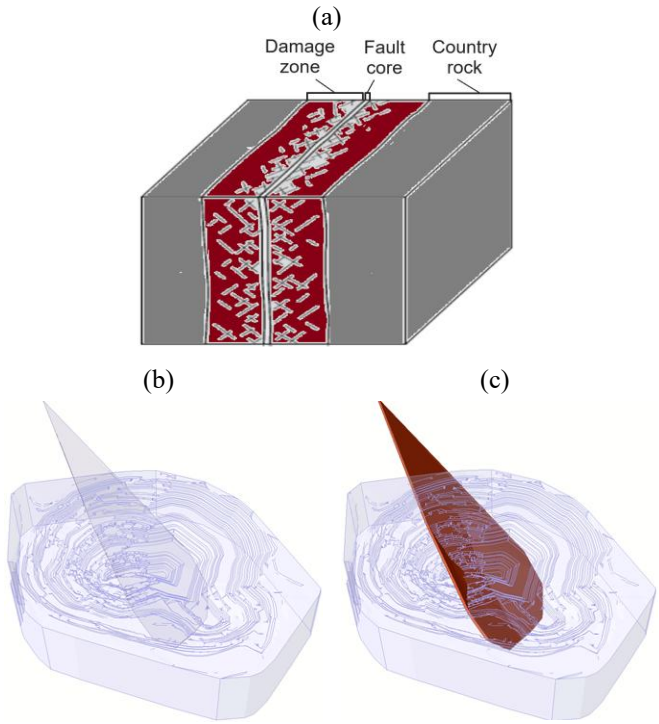

Figure 5. Creating volume for filling with a fracture system: (a) schematic representation of the fault core and the zone of disturbed rocks; (b) adding a fault plane to the model; (c) "extruding" the plane to a width of 30 m to obtain a zone of intense fracturing

In accordance with the work [38], the fault zone can be divided into the fault core, the damage zone, and the protolith. Most of the displacement is concentrated in the fault core, where intense fracturing, breccia formation and geochemical changes are observed. In most cases, the fault core is a cavity filled with clay material. The adjacent fault zone is a network of secondary fractures, veins and small faults. The protolith or host rock shows virtually no signs of brittle deformation, with the exception of fractures. Fault cores are zones of damage, that is, structures of about 1.0 m thick, consisting of fractures filled with clay material and smaller faults. Damage zones often have rather asymmetrical thickness within individual fault zones [39].

To model the corresponding volume that will be filled with the fracture system, RS3 provides an operation "Extrude", which adds the w parameter to the model geometry, characterizing the actual width of the fault zone. In our research, in accordance with geologic service data, the w parameter is taken to be equal to 30 m. A test model implementing the idea of "extrusion" is shown in Figure 5c. To create the fracture system, the RS3 option "Discrete Fracture Networks" was used, which allows modelling contact between elements taking into account the fault structure and provides both sliding between the fault boundaries and the main mass, as well as sliding inside the fracture system. Fracture systems are implemented in a volume with a width w, which is controlled by the RS3 DFN Control Volume option.

The edges of fractures are characterized by their openness, type of filler and the roughness of the walls. These fracture features are modelled using the Discreet Fracture Networks tool, which involves parameters such as normal k_n and shear k_s fracture stiffness. For the conditions of the Kacharsky quarry, setting these parameters is a rather complex

task, since there is limited access to the rocks that fill the geological faults located in the bottom part of the quarry. According to the geological service data, the core of the fault is filled with breccia, which is a conglomerate of fragmentary rocks (quartz, limestone, calcite, clay minerals), partially cemented. Damaged rock zone is a limestone heavily disturbed by fracture systems. The fractures are filled with secondary calcite crystals. Even if a certain rock volume can be extracted by drilling, it is difficult to conduct standard tests, since determining the rock properties using direct methods requires a large number of samples of the correct shape. Making such samples from breccia is practically impossible because it is a weak material and the samples can be damaged when cutting, shaping and grinding of the surfaces [40]. For this reason, assessing the strength properties of fault breccia using indirect methods in accordance with its texture is the most accessible approach. In particular, the assessment of the rock mass "quality" in accordance with the RMR (Rock Mass Rating) and GSI (Geological Strength Index), as well as the introduction of the structural weakening coefficient [35] into the calculation, can be performed to assess the deformation properties of the fractured medium. For cemented rock inside the fault, the GSI index is assessed to be 25-35, and for uncemented rock, the GSI is assessed to be 15-25. By analogy with [41], in this work, for fractured sandstone, we assume GSI = 20. Then, using the recommendations in [42], the rock stress-strain modulus E_f in the fault zone can be estimated using the Formula:

$$E_f = E_0\left(0.02 + \frac{1}{1+e^{60-\mathrm{GSI}/11}}\right), \quad (2)$$

where:

E_0 – average rock stress-strain modulus outside the fault zone.

Then E_f = 4.6 GPa · 0.05 = 0.23 GPa (since $E_f / E_0 = 0.05$ for GSI = 20). For fractures with an opening of h = 0.01-0.1 m, a normal stiffness of no more than $k_n = E_f / 0.1$ = 2.3 GPa/m should be specified. Shear stiffness is assumed to be equal to $k_s = 0.1 \cdot k_n$ = 0.23 GPa/m.

In reality, the mass structure in the bottom part of the Kacharsky quarry is very complex, with a system of intersecting disturbances (Fig. 6). Each of them is modelled as described above, that is, as a separate volume filled with fractured material. This model implements a system of three intersecting fracture systems identified during the geological exploration stage.

The configuration of the fault planes changes slightly when removing the next steeply sloping layer. The model, including faults, is created for each stage of mining in accordance with the actual geometry of the weakening plane.

3. Results and discussion

3.1. Model without faults

It was mentioned above that the starting point for the simulation is the creation of a homogeneous rock mass model with averaged properties, without simulating rock layers and faults. During the first two stages of mining, when the first two layers are removed, the quarry walls are quite stable, as loose overburden is removed during these stages and the slope angle of the walls does not exceed 15°. Safety factor (FoS or SRF) is 2.6, which is twice the standard value recommended for the planning of ore quarries [43].

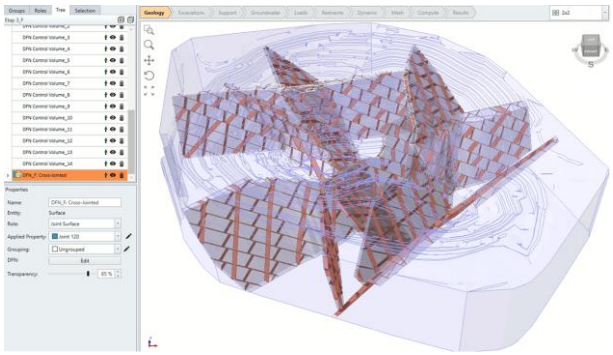

Figure 6. Visualization of a model with disturbed zones near fault planes

A slight decrease in SRF begins at stage #3 when the slope angle of the walls increases to 17° and the quarry depth reaches 27 m. At this stage, the safety factor is SRF = 2.52 (Fig. 7), and the largest potential shear strains and total displacements are formed in the eastern and north-eastern sectors of the quarry.

According to the shear strength reduction procedure, the fact that the safety factor is 2.52 means that slope stability will only be lost if the strength parameters (cohesion, internal friction angle) decrease by 2.52 times. In this case, a potential sliding surface is formed (red colour in Fig. 7b), where potential maximum shear strains γ are realized, as well as maximum displacements U.

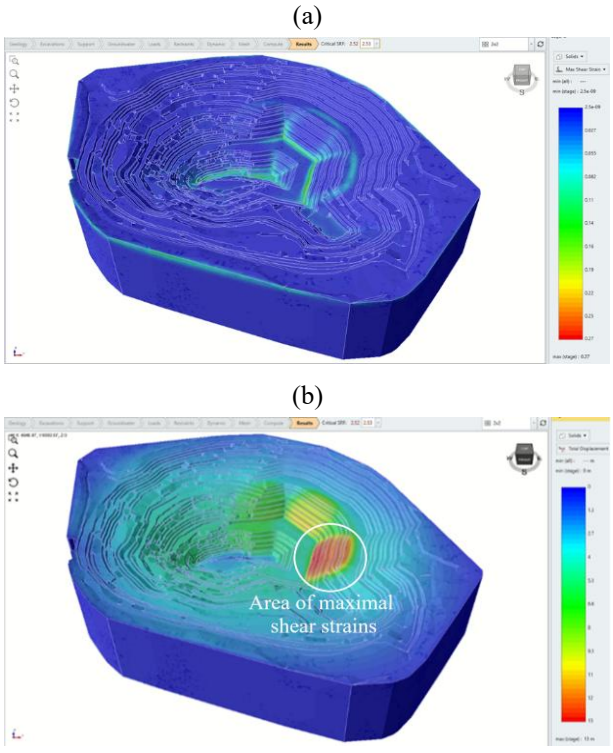

Figure 7. Results of finite element modelling for a homogeneous model at stage #3 (without taking into account faults and fracturing): (a) maximum shear strains; (b) maximum total displacements

In the absence of complicating factors such as faults, the sliding surface at stage #3 of mining is local, although the maximum shear strains γ reach values of 0.05-0.11 (Fig. 7a). The total displacements U in the area highlighted in Figure 7b could potentially develop to a value of 9-12 m.

3.2. Influence of faults

The presence of tectonic faults in the bottom part of the quarry (Fig. 8) has a significant influence on the rock SSS even at the above-discussed stage #3 of mining, when only loose overburden is actually removed. Modelling of weakening planes led to a decrease in the minimum SRF of the quarry wall at stage #3 from 2.52 (no-fault model) to 1.91 (model with faults, Fig. 8a), that is, by 24%.

(a)

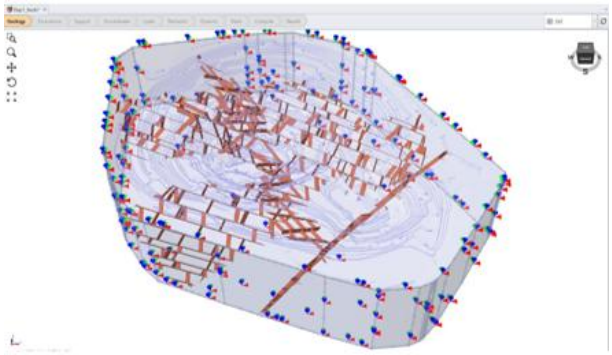

(b)

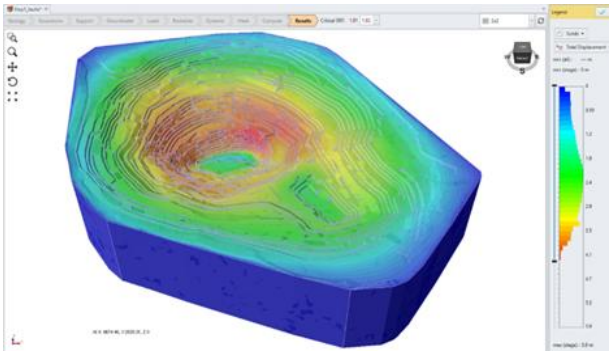

Figure 8. Determination of SSS and SRF taking into account faults (stage #3 of mining): (a) designed scheme; (b) potential rock displacements in the quarry walls at a safety factor of 1.91

In this case, it is impossible to identify a local sliding surface with the greatest displacements on the 3D model of the entire quarry bowl. It can be said that the wall stability is reduced along the entire perimeter compared to the model without faults.

We cut the model in north-south (Fig. 9a) and east-west (Fig. 9b) directions to show the distribution of displacements in detail. A model section in the east-west direction (Fig. 9b) showed that the largest potential displacements in this section are $U = 3.2$ m, and their distribution is such that it is impossible to clearly identify the potential sliding surface. Larger potential displacements of $U = 5.9$ m were noted when the model was sectioned by a "north-south" plane. They are located in the northern part of the wall, where the sliding surface is clearly visible.

This calculation result is confirmed by data from in-situ observations of the near-wall mass state, conducted when the quarry depth was 270 m, that is, at stage #3 of mining. In the northern part of the quarry, deformation zones were recorded (Fig. 10) extending 550 m along the front, where fractures developed on the surface of the benches. In addition, a subsidence of ramps and service roads occurred by up to 5 m.

(a)

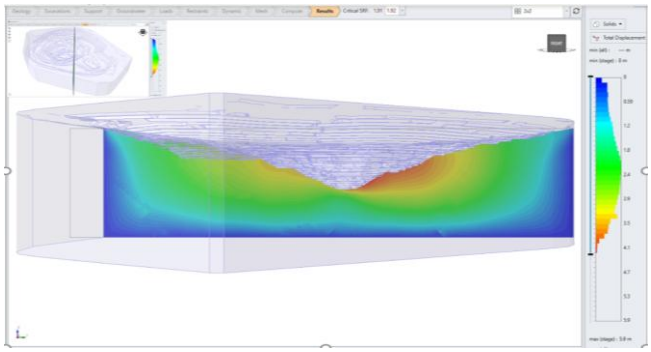

(b)

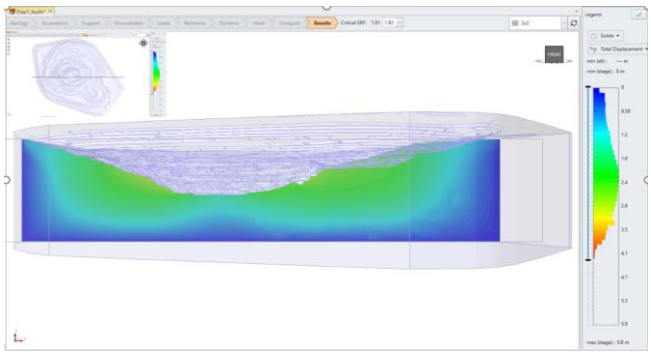

Figure 9. Potential rock displacements in the diametric sections of the quarry (stage #3): (a) model section with a north-south plane; (b) model section with an east-west plane

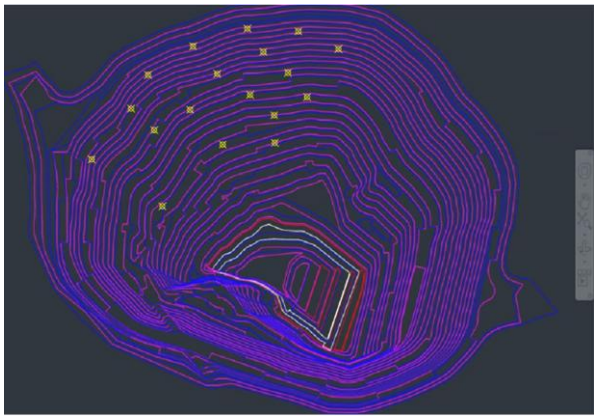

Figure 10. Deformation zones along the Kacharsky quarry walls

The digital model of the quarry wall and the weakening planes in its bottom part at stages #4 and 5 of mining remains almost unchanged compared to stage #3, since the deepening of the quarry and the change in the line of benches during this period are not significant. However, increasing the quarry depth to 390 m and the corresponding increase in the average wall slope angle along the perimeter to 20° causes a decrease in the safety factor to 1.62 at stage #4 and to 1.55 at stage #5. The stability drop is 15% at stage #4 compared to stage #3 and 4.3% at stage #5 compared to stage #4. At stages #4 and 5, the 3D model of the entire quarry bowl including faults in the bottom part, demonstrates the equal possibility of realizing shear along the perimeter of the quarry. The model sectioned with radial planes (Fig. 11) shows the formation of potential sliding surfaces in each section, where displacements of 4-5 m can occur with a potential reduction in strength properties by 1.62-1.55.

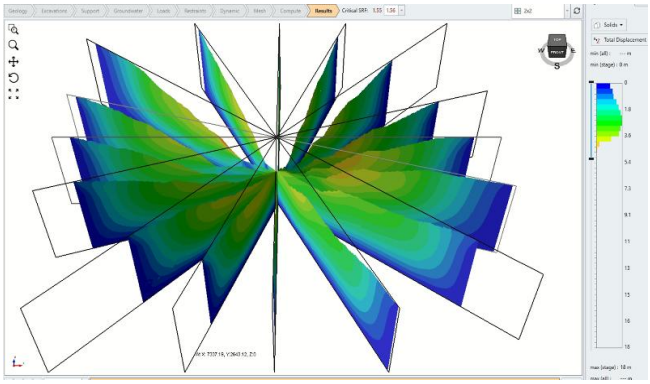

Figure 11. Distribution of rock displacements in radial sections (stage #5)

At subsequent stages of mining, the deepening of the quarry and the change in the line of benches make a difference in the distribution of displacements and the wall stability. The most important factor is assessing the wall stability at the final stage of ore mining, when the planned depth of the quarry (570 m) is reached. At this stage, the average wall slope angle along the perimeter is 30°.

It should be noted that the SSS simulation based on a homogeneous model without taking into account the influence of faults [44] gives a stability prediction at the level of FoS = 1.53 (Fig. 12a). From this, it is concluded that the quarry walls are stable at the final stage of mining, because the FoS does not fall below a level recommended by project standards $SoF_n = 1.3$. However, this prediction may be overly optimistic, as it does not take into account the influence of the weakening surfaces on the rock SSS in the quarry bottom part. Modelling of faults at the final stage of quarry deepening (Fig. 12b) shows that the safety factor of a steeply sloping wall in a structurally disturbed rock mass decreases to the value FoS = 1.1 and becomes less than the recommended value $SoF_n = 1.3$.

Thus, at the final stage of mining, when the planned depth of the quarry is reached, the fault presence causes a decrease in the stability of the quarry walls to a level of SoF = 1.1, which is less than the safety factor recommended by project standards. In addition, fault accounting shows that the greatest shear strains, and therefore absolute displacements, can occur at the final 25 stage rather on the eastern quarry wall than on the southern wall, as predicted without taking fault lines into account.

A summary of the results on the reduction in wall stability as the quarry deepens is presented in Figure 13, which indicates the stages of mining and the corresponding resulting slope angles of the quarry walls.

Analysis of the generalized graph shows that modelling of faults in the bottom part of the quarry gives a stability estimate (FoS or SRF), which is 24-32% lower than that obtained without taking faults into account.

3.3. Model sensitivity analysis

A problematic stage of modelling is the assignment of physical-mechanical properties to the material located in the fault zone. It was mentioned above that the influence of a fault on the adjacent rock SSS is determined by the physical-mechanical properties of the material in the fault zone, and how these properties correlate with the properties of the entire rock mass.

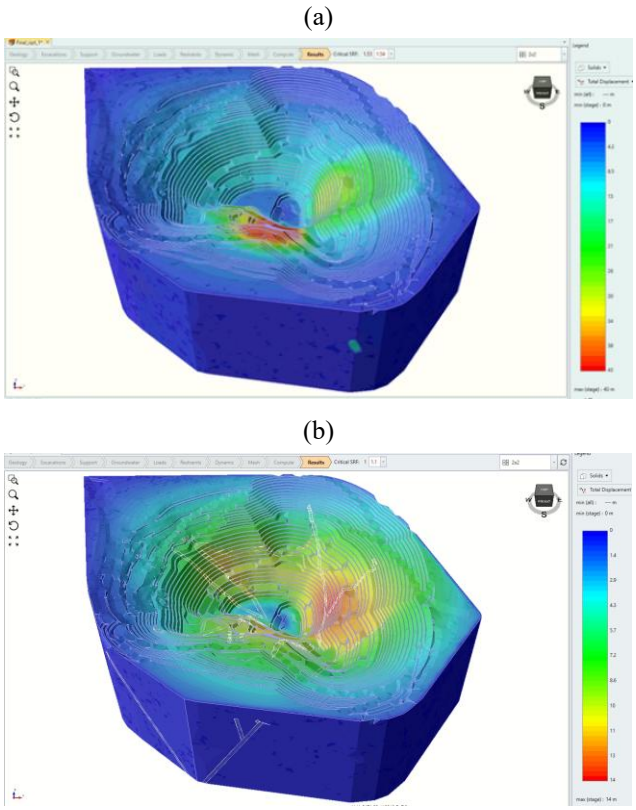

Figure 12. Distribution of displacements in the quarry walls at stage #25: (a) homogeneous model without considering faults; (b) distribution of displacements in the walls, taking into account faults

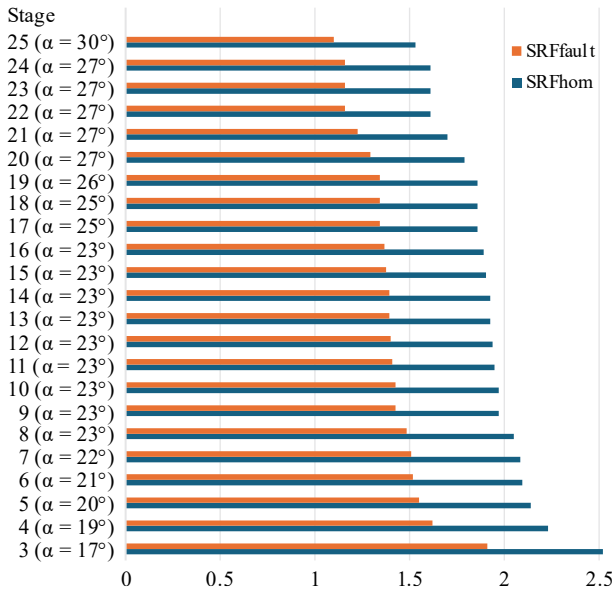

Figure 13. Diagram showing the reduction in safety factor at all stages of mining: SRFhom – safety factor calculated for a homogeneous mass; SRFfault – safety factor calculated taking into account faults

In this case, a key role is played by the stiffness ratio of mentioned rock mass parts, which is reduced to the ratio of elastic modules $E_r = E_f / E_0$.

When modelling faults in the bottom part of the quarry, this ratio was assumed to be 0.05, which in turn determined the normal and shear stiffness of the fracture-filling material: $k_n = 2.3$ GPa/m; $k_s = 0.23$ GPa/m. To assess the in-

fluence of these characteristics on the occurrence of shear strains and, consequently, on the formation of sliding surfaces, the fault was modelled in a 2D setting (Fig. 14) using RS2 Rocscience software. The fault boundary is simulated with a fracture characterized by normal stiffness k_n and tangential stiffness k_s, and the fault zone is simulated by specifying a strain modulus E_f, which is reduced relative to the elastic modulus of surrounding rock mass E_0. The ratio of $E_r = E_f / E_0$ varied in calculations from 0.05 to 2.0, normal stiffness varied from 2.0 to 200 GPa/m, and tangential stiffness took values from 0.2 to 20 GPa/m, respectively. This simulated various degrees of fracture opening, bordered the fault zone.

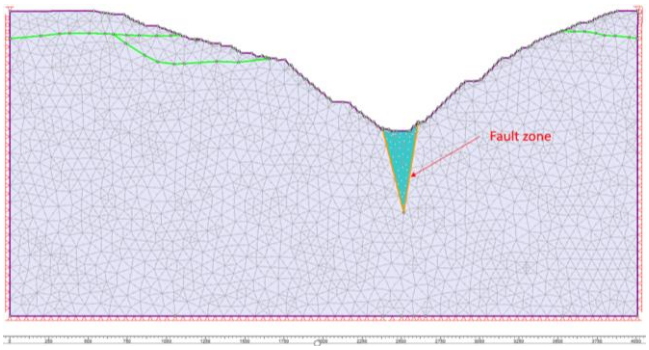

Figure 14. Designed scheme for modelling a fault in 2D

The distribution of maximum shear strains and displacement vectors (Fig. 15) confirm that in the fault zone there is a tendency for extruding disintegrated rock mass into the mined-out space under the action of shear stresses.

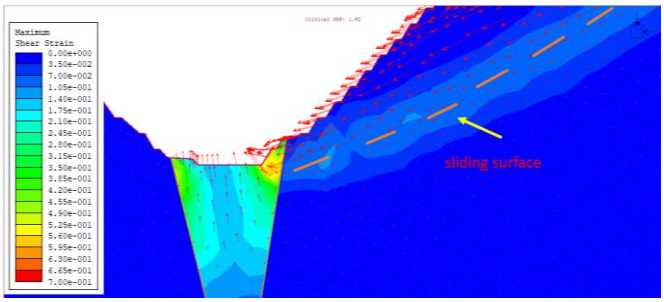

Figure 15. Distribution of maximum shear strains and displacement vectors

Multivariate simulations showed that shear strains are greater, the lower the stiffness of the fracture-filling material (Fig. 16) and the lower the ratio E_r. In the range of changes in the k_n argument up to 2.5 GPa/m, the difference in the realized shear strains is the most significant. When reducing the stiffness of the material inside the fault zone from $E_r = 0.2$ to $E_r = 0.05$, the maximum shear strains in the bottom part of the quarry increase from 0.05 to 0.075, that is by 50%.

Thus, the maximum strain values depend on how weak and disintegrated the material is in the fault zone. Therefore, in order to adequately model the state of deep quarry walls in the absence of complete information about the properties of rocks inside the fault zone, it is necessary to focus on the lower normal stiffness of the fracture-filling material (no more than 2.5 GPa/m) and a lower rock stiffness in the fault zone, characterized by E_r value of no more than 0.05.

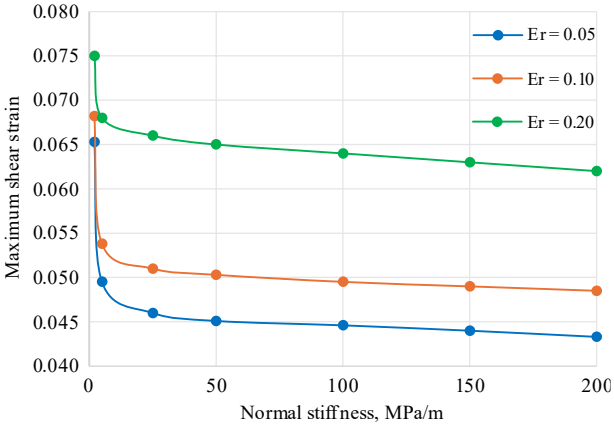

Figure 16. Change in maximum shear strains in the bottom part of the quarry depending on the normal stiffness of the fracture-filling material and the ratio $E_r = E_f / E_0$

In general, accounting for the characteristics of geological faults, such as openness, contact filler type, and fracture surface roughness, is a complex task in geomechanics and at this stage is accomplished by selecting the normal and shear stiffness of the contact, modelling the interaction between the fracture-fault and the main rock mass. The algorithm for selecting contact parameters should be improved, considering surveyor observation data of the fault state in the event of its outcrop to the surface.

Another way to improve the reliability of mathematical modelling is to modify well-known strength criteria based on the development of ideas about processes of soil and rock mass shear. In particular, the Mohr-Coulomb criterion can be improved, as shown in [45], by taking into account the influence of the stress state of rocks on their plastic deformation potential.

It should also be noted that the reliability of modelling the soil-rock mass SSS and assessing the stability of quarry walls is quite difficult to confirm through observations, instrumental measurements or special experiments. The exception is cases of obvious stability loss, which can serve as a basis for solving the inverse problem and, consequently, for calibrating the constitutive model of the medium. However, a more promising approach appears to be the comprehensive and complementary use of mathematical modelling and geophysical methods, in particular acoustic emission analysis and seismoacoustic prediction. In [46], it is noted that rough fault surfaces, characterized by the presence of depressions and protrusions, cause stress concentration and energy accumulation, leading to local failure in the upper and lower fault blocks. Various failure modes are possible here, provoking the activation of the fault. Monitoring of acoustic emission in these areas can be an effective method for identifying fault activation. The current seismoacoustic prediction [47] can also provide timely information on the evolution of fault characteristics in the mining process, with appropriate adaptation of existing methods.

4. Conclusions

FEM-analysis of the stress-strain state of the Kacharsky quarry walls at various stages of mining, taking into account faults in its bottom part, provides a safety factor (FoS) that is 24-32% lower than that obtained without taking faults into account.

Modelling faults using RS3 software involves specifying the relevant volume, which is filled with a fracture system ("Extrude" operation). To do this, parameter w is added to the model geometry, characterizing the actual fault zone width, and which, according to geological service data from the Kacharsky quarry, is assumed to be 30 m. To create the fracture system, the RS3 "Discrete Fracture Networks" option was used, which allows modelling contact between elements taking into account the fault structure and provides both sliding between the fault boundaries and the main mass, and sliding inside the fracture system.

The fracture properties are modelled using parameters such as normal k_n and shear k_s fracture stiffness, which are determined using mass quality indicators (GSI) inside the fault zone. Parametric analysis shows that in the range of argument changes $k_n < 2.5$ GPa/m, the difference in the realized shear strains is the most significant. When reducing the Er index, which characterizes the ratio of material stiffness inside and outside the fault zone, from $E_r = 0.2$ to $E_r = 0.05$, the maximum shear strains in the bottom part of the quarry increase from 0.05 to 0.075, that is, by 50%. Thus, the disintegrated medium in the fault zone provokes the development of shear strains.

In general, accounting for the characteristics of geological faults, such as openness, contact filler type, and fracture surface roughness, is a complex task in geomechanics and at this stage is accomplished by selecting the normal and shear stiffness of the contact, modelling the interaction between the fault and the main rock mass. The algorithm for selecting contact parameters should be improved, considering surveyor observation data of the fault state in the event of its outcrop to the surface. To adequately model the state of deep quarry walls in the absence of complete information about the properties of rocks inside the fault zone, it is necessary to focus on the lower normal stiffness of the fracture-filling material (no more than 2.5 GPa/m) and a lower rock stiffness in the fault zone, characterized by E_r value of no more than 0.05.

Author contributions

Conceptualization: SM, OS; Data curation: AM; Formal analysis: ZS; Funding acquisition: SM, AB; Investigation: AM, DB, OS, AB; Methodology: DB, OS; Project administration: SM, ZS; Resources: SM; Software: AM, DB; Supervision: AM, SM; Validation: AB, ZS; Visualization: ZS; Writing – original draft: AM, DB, OS, ZS; Writing – review & editing: SM, OS, AB. All authors have read and agreed to the published version of the manuscript.

Funding

This work is funded by the Ministry of Education and Science of the Republic of Kazakhstan, grant No. AP26198535.

Acknowledgements

The authors gratefully acknowledge the academic support, constructive discussions, and professional guidance provided by colleagues and reviewers, which significantly contributed to improving the quality and clarity of this study.

Conflicts of interests

The authors declare no conflict of interest.

Data availability statement

The original contributions presented in the study are included in the article, further inquiries can be directed to the corresponding author.

References

[1] Sdvyzhkova, O., Moldabayev, S., Bascetin, A., Babets, D., Kuldeyev, E., Sultanbekova, Zh., Amankulov, M., & Issakov, B. (2022). Probabilistic assessment of slope stability at ore mining with steep layers in deep open pits. *Mining of Mineral Deposits*, *16*(4), 11-18. https://doi.org/10.33271/mining16.04.011

[2] Bazaluk, O., Petlovanyi, M., Sai, K., Chebanov, M., & Lozynskyi, V. (2024). Comprehensive assessment of the earth's surface state disturbed by mining and ways to improve the situation: case study of Kryvyi Rih Iron-ore Basin, Ukraine. *Frontiers in Environmental Science*, *12*, 1480344. https://doi.org/10.3389/fenvs.2024.1480344

[3] Sloan, S.W. (2013). Geotechnical stability analysis. *Géotechnique*, *63*(7), 531-571. https://doi.org/10.1680/geot.12.rl.001

[4] Bazaluk, O., Anisimov, O., Saik, P, Lozynskyi, V., Akimov, O., & Hrytsenko, L. (2023). Determining the safe distance for mining equipment operation when forming an internal dump in a deep open pit. *Sustainability*, *15*(7), 5912. https://doi.org/10.3390/su15075912

[5] Babets, D.V., Sdvyzhkova, O.O., Larionov, M.H., & Tereshchuk, R.M. (2017). Estimation of rock mass stability based on probability approach and rating systems. *Naukovyi Visnyk Natsionalnoho Hirnychoho Universytetu*, *2*, 58-64.

[6] Kruszewski, M., Klee, G., Niederhuber, T., & Heidbach, O. (2022). In situ stress database of the greater Ruhr region (Germany) derived from hydrofracturing tests and borehole logs. *Earth System Science Data*, *14*(12), 5367-5385. https://doi.org/10.5194/essd-14-5367-2022

[7] Li, P., Cai, M., Gorjian, M., Ren, F., Xi, X., & Wang, P. (2023). Interaction between in situ stress states and tectonic faults: A comment. *International Journal of Minerals, Metallurgy and Materials*, *30*(7), 1227-1243. https://doi.org/10.1007/s12613-023-2607-8

[8] Reiter, K. (2021). Stress rotation – impact and interaction of rock stiffness and faults. *Solid Earth*, *12*(6), 1287-1307. https://doi.org/10.5194/se-12-1287-2021

[9] Liu, J., Yang, H., Xu, K., Wang, Z., Liu, X., Cui, L., Zhang, G., & Liu, Y. (2022). Genetic mechanism of transfer zones in rift basins: Insights from geomechanical models. *GSA Bulletin*, *134*(9-10), 2436-2452. https://doi.org/10.1130/b36151.1

[10] Qian, D., Zhang, N., Zhang, M., Shimada, H., Cao, P., Chen, Y., Wen, K., Yang, S., & Zhang, N. (2017). Application and evaluation of ground surface pre-grouting reinforcement for 800-m-deep underground opening through large fault zones. *Arabian Journal of Geosciences*, *10*(13), 285. https://doi.org/10.1007/s12517-017-3052-7

[11] Childs, C., Manzocchi, T., Walsh, J.J., Bonson, C.G., Nicol, A., & Schöpfer, M.P.J. (2009). A geometric model of fault zone and fault rock thickness variations. *Journal of Structural Geology*, *31*(2), 117-127. https://doi.org/10.1016/j.jsg.2008.08.009

[12] Wyllie, D.C., & Mah, C.W. (2017). *Rock slope engineering*. London, United Kingdom: CRC Press, 456 p. https://doi.org/10.1201/9781315274980

[13] Pariseau, W.G., Puri, S., & Schmelter, S.C. (2008). A new model for effects of impersistent joint sets on rock slope stability. *International Journal of Rock Mechanics and Mining Sciences*, *45*(2), 122-131. https://doi.org/10.1016/j.ijrmms.2007.05.001

[14] You, G., Jaggi, N., Al Mandalawi, M., Dowling, K., & Dahlhaus, P. (2018). Effect of faults on stability of partially saturated rock slope. *Deep Rock Mechanics: From Research to Engineering*, 393-402. https://doi.org/10.1201/9781351042666-39

[15] Al Heib, M., Zevgolis, I.E., Theocharis, A.I., Koukouzas, N.C., & Coccia, S. (2021). Analysis of faults' effect on the stability of surface lignite mining areas using the distinct element method. *Geotechnical and Geological Engineering*, *40*(3), 1307-1321. https://doi.org/10.1007/s10706-021-01964-z

[16] Kimura, N., Matsuki, K., Nakama, S., & Sato, T. (2003). Estimation of regional stress for heterogeneous rock mass. *Shigen-to-Sozai*, *119*(10, 11), 655-662. https://doi.org/10.2473/shigentosozai.119.655

[17] Tonon, F., & Asadollahi, P. (2008). Validation of general single rock block stability analysis (BS3D) for wedge failure. *International Journal of Rock Mechanics and Mining Sciences*, *45*(4), 627-637. https://doi.org/10.1016/j.ijrmms.2007.08.014

[18] Rong, S., & Wang, J. (2024). Study on the influence of multiple faults on the stability of high and steep slopes in open-pit mines. *Energy Power and Automation Engineering*, 799-814. https://doi.org/10.1007/978-981-99-8878-5_78

[19] Liu, H., Si, H., Yang, Z., & Xu, D. (2025). Stress redistribution and crack evolution during fault slip: Insights from coupled finite-discrete element method simulations. *Physics of Fluids*, *37*(5), 056626. https://doi.org/10.1063/5.0270195

[20] Yin, H., Li, X., Su, T., Xu, Y., Yuan, X., Liu, J., & Wei, N. (2025). A study on the variation characteristics of floor fault activation induced by mining. *Applied Sciences*, *15*(16), 8811. https://doi.org/10.3390/app15168811

[21] Vavryčuk, V. (2014). Iterative joint inversion for stress and fault orientations from focal mechanisms. *Geophysical Journal International*, *199*(1), 69-77. https://doi.org/10.1093/gji/ggu224

[22] Hui, Q., Gao, F., Tan, X., & You, D. (2023). Determining tunnel stability across fault zones under seismic loading based on load/unload response ratio theory. *Journal of Vibroengineering*, *25*(7), 1285-1304. https://doi.org/10.21595/jve.2023.23284

[23] Saik, P., Rysbekov, K., Kassymkanova, K. K., Lozynskyi, V., Kyrgizbayeva, G., Moldabayev, S., Babets, D., & Salkynov, A. (2024). Investigation of the rock mass state in the near-wall part of the quarry and its stability management. *Frontiers in Earth Science*, *12*, 1395418. https://doi.org/10.3389/feart.2024.1395418

[24] Petlovanyi, M., Sai, K., Malashkevych, D., Popovych, V., & Khorolskyi, A. (2023). Influence of waste rock dump placement on the geomechanical state of underground mine workings. *IOP Conference Series: Earth and Environmental Science*, *1156*(1), 012007. https://doi.org/10.1088/1755-1315/1156/1/012007

[25] Sdvyzhkova, O., Moldabayev, S., Babets, D., Bascetin, A., Asylkhanova, G., Nurmanova, A., & Prykhodko, V. (2024). Numerical modelling of the pit wall stability while optimizing its boundaries to ensure the ore mining completeness. *Mining of Mineral Deposits*, *18*(2), 1-10. https://doi.org/10.33271/mining18.02.001

[26] Saik, P., Cherniaiev, O., Anisimov, O., & Rysbekov, K. (2023). Substantiation of the direction for mining operations that develop under conditions of shear processes caused by hydrostatic pressure. *Sustainability*, *15*(22), 15690. https://doi.org/10.3390/su152215690

[27] Deng, D., Li, L., & Zhao, L. (2017). Limit equilibrium method (LEM) of slope stability and calculation of comprehensive factor of safety with double strength-reduction technique. *Journal of Mountain Science*, *14*(11), 2311-2324. https://doi.org/10.1007/s11629-017-4537-2

[28] Li, Y., Yu, L., Song, W., & Yang, T. (2019). Three-dimensional analysis of complex rock slope stability affected by fault and weak layer based on FESRM. *Advances in Civil Engineering*, *2019*(1). https://doi.org/10.1155/2019/6380815

[29] Barton, N. (2013). Shear strength criteria for rock, rock joints, rockfill and rock masses: Problems and some solutions. *Journal of Rock Mechanics and Geotechnical Engineering*, *5*(4), 249-261. https://doi.org/10.1016/j.jrmge.2013.05.008

[30] Wibberley, C.A.J., Yielding, G., & Di Toro, G. (2008). Recent advances in the understanding of fault zone internal structure: A review. *Geological Society, London, Special Publications*, *299*(1), 5-33. https://doi.org/10.1144/sp299.2

[31] Treffeisen, T., & Henk, A. (2020). Faults as volumetric weak zones in reservoir-scale hydro-mechanical finite element models – A comparison based on grid geometry, mesh resolution and fault dip. *Energies*, *13*(10), 2673. https://doi.org/10.3390/en13102673

[32] Henk, A. (2020). Numerical modelling of faults. *Understanding Faults*, 147-165. https://doi.org/10.1016/b978-0-12-815985-9.00004-7

[33] Hergert, T., Heidbach, O., Reiter, K., Giger, S.B., & Marschall, P. (2015). Stress field sensitivity analysis in a sedimentary sequence of the Alpine foreland, northern Switzerland. *Solid Earth*, *6*(2), 533-552. https://doi.org/10.5194/se-6-533-2015

[34] Reiter, K., Heidbach, O., & Ziegler, M.O. (2024). Impact of faults on the remote stress state. *Solid Earth*, *15*(2), 305-327. https://doi.org/10.5194/se-15-305-2024

[35] Sdvyzhkova, O., Moldabayev, S., Babets, D., Kovrov, O., & Adil, T. (2021). Numerical simulation of the open pit stability based on probabilistic approach. *Naukovyi Visnyk Natsionalnoho Hirnychoho Universytetu*, *6*, 29-34. https://doi.org/10.33271/nvngu/2021-6/029

[36] Teng, L., He, Y., Wang, Y., Sun, C., & Yan, J. (2024). Numerical stability assessment of a mining slope using the synthetic rock mass modeling approach and strength reduction technique. *Frontiers in Earth Science*, *12*, 1438277. https://doi.org/10.3389/feart.2024.1438277

[37] Chen, T., Xu, G., Li, C., Peng, H., & Wang, B. (2024). Reactivation mechanism of a deep-seated landslide along fault zones in Baihetan reservoir area. *Bulletin of Engineering Geology and the Environment*, *83*(12), 487. https://doi.org/10.1007/s10064-024-03998-y

[38] Faulkner, D.R., Mitchell, T.M., Jensen, E., & Cembrano, J. (2011). Scaling of fault damage zones with displacement and the implications for fault growth processes. *Journal of Geophysical Research*, *116*(B5). https://doi.org/10.1029/2010jb007788

[39] Laurita, S., Agosta, F., Cavalcante, F., Rustichelli, A., & Giorgioni, M. (2016). Shearing of syn-sedimentary carbonate breccia along strike-slip faults, Altamura Fm., Southern Italy. *Italian Journal of Geosciences*, *135*(1), 41-54. https://doi.org/10.3301/ijg.2014.37

[40] Usenov, Kz., Kuvakov, Sz., Alibaev, A., Kuvakov, Z., & Takeeva, A. (2022). The change in physical and mechanical properties of rocks in the course of mining in Makmal Mine. *IOP Conference Series: Earth and Environmental Science*, *991*(1), 012016. https://doi.org/10.1088/1755-1315/991/1/012016

[41] Aitkazinova, S., Sdvyzhkova, O., Imansakipova, N., Babets, D., & Klymenko, D. (2022). Mathematical modeling the quarry wall stability under conditions of heavily jointed rocks. *Naukovyi Visnyk Natsionalnoho Hirnychoho Universytetu*, *6*, 18-24. https://doi.org/10.33271/nvngu/2022-6/018

[42] Marinos, P., & Hoek, E. (2000). GSI: A geologically friendly tool for rock mass strength estimation. *ISRM International Symposium*.

[43] SOU-N MPP 73.020-078-1:2007. (2007). *Standards of technological design for mining enterprises using an open method of developing mineral deposits*. Kyiv, Ukraine: Ministry of Industrial Policy of Ukraine.

[44] Moldabayev, S., Sdvyzhkova, O., Babets, D., Amankulov, M., & Nurmanova, A. (2024). Numerical simulation of a pit wall stability considering seismic impact in terms of ultra-deep open-pit mine. *Geomining*, 121-134. https://doi.org/10.1007/978-3-031-70725-4_9

[45] Sdvyzhkova, O.O., Olishevska, S.O., Shashenko, O.M., & Morklyanyk, B.V. (2025). Analysis of a soil slope stability based on modified failure criterion. *Naukovyi Visnyk Natsionalnoho Hirnychoho Universytetu*, *4*, 90-97. https://doi.org/10.33271/nvngu/2025-4/090

[46] Sdvyzhkova, O., Golovko, Y., & Klymenko, D. (2017). Effect of harmonic oscillations on a crack initiation in the rock mass. *Naukovyi Visnyk Natsionalnoho Hirnychoho Universytetu*, *4*, 13-18. https://doi.org/10.15407/mining10.02.072

[47] Zhao, Q., Zhao, Y., Yang, T., & Wang, S. (2025). Mechanical behavior and micro-crack propagation mode of fault stick-slip under various roughness conditions. *Geomechanics and Geophysics for Geo-Energy and Geo-Resources*, *11*(1), 1. https://doi.org/10.1007/s40948-024-00920-4

Чисельне моделювання стійкості бортів кар'єру з урахуванням локалізації геологічних розломів у донній частині

А. Молдабаєв, Д. Бабець, С. Молдабаєв, О. Сдвижкова, А. Баскетін, Ж. Султанбекова

Мета. Оцінка впливу геологічних порушень, розташованих у донній частині надглибокого рудного кар'єру Качарський, на напружено-деформований стан (НДС) його бортів та визначення запасу їх стійкості з урахуванням ускладненої геологічної ситуації.

Методика. Методика моделювання площин розлому ґрунтується на 3D скінчено-елементному аналізі засобами програмного продукту RS3 Rocscience. Зона розлому представлена середовищем із системою тріщин. Характеристики тріщин, такі як ступінь розкриття, тип наповнювача контакту, якість поверхонь, здійснюється за рахунок підбору нормальної та зсувної жорсткості контакту. Міцнісні та деформаційні властивості гірської породи всередині зони розлому регламентуються малими значеннями геологічного індексу (GSI = 20), що відповідають за класифікацією Хоека-Брауна масиву "поганої" якості. Основний масив поза зоною розлому представлений пружно-пластичним середовищем, де перехід у непружну стадію деформування визначається критерієм міцності Кулона-Мора.

Результати. МКЕ-аналіз напружено-деформованого стану бортів кар'єру Качарський на різних етапах розробки з урахуванням розломів у його донній частині дає оцінку стійкості (SF), яка на 28-30% нижча за ту, що отримана без урахування розломів. Параметричний аналіз показав, що при значеннях нормальної жорсткості матеріалу-заповнювача тріщин до 2.5 ГПа/м різниця у реалізованих зсувних деформаціях найбільш істотна. При зменшенні показника E_r, що характеризує співвідношення жорсткостей матеріалів усередині та поза зоною розлому від значення $E_r = 0.2$ до $E_r = 0.05$, максимальні зсувні деформації в донній частині кар'єру

збільшуються від 0.05 до 0.075, тобто на 50%. Таким чином, більш слабке та дезінтегроване середовище в зоні розлому провокує розвиток зсувних деформацій і зумовлює зниження стійкості борту.

Наукова новизна. Вперше для реальних гірничо-геологічних умов глибокого рудного кар'єру встановлена закономірність зміни запасу міцності крутих бортів з урахуванням геологічних розломів у донній частині кар'єру. Встановлено залежність зсувних деформацій від показника нормальної жорсткості тріщин та співвідношення модулів деформації породного середовища всередині зони розлому та поза нею.

Практична значимість. Значення коефіцієнта стійкості бортів на кожному етапі розробки є ключовим параметром для прийняття технологічних рішень і регламентів. Встановлений факт зниження стійкості бортів на останньому етапі розробки до критичного рівня (SF = 1.1) через присутність розломів може бути основою для перегляду технологічної схеми видобутку руди на фінальній стадії, зокрема, може бути прийнято рішення зменшити кут укосу уступів.

Ключові слова: *геологічний розлом; відкрита гірнича виробка; глибокий кар'єр; стійкість укосу; чисельне моделювання*

Publisher's note

All claims expressed in this manuscript are solely those of the authors and do not necessarily represent those of their affiliated organizations, or those of the publisher, the editors and the reviewers.